JACS Au
AN OPEN ACCESS JOURNAL OF THE AMERICAN CHEMICAL SOCIETY

pubs.acs.org/jacsau
Article

Optical Control of Microtubule Accumulation and Dispersion by Tau-Derived Peptide-Fused Photoresponsive Protein

Soei Watari, Hiroshi Inaba,* Qianru H. Lv, Muneyoshi Ichikawa,* Takashi Iwasaki, Bingxun Wang, Hisashi Tadakuma, Akira Kakugo, and Kazunori Matsuura*

Cite This: JACS Au 2025, 5, 791−801
Read Online

ACCESS | Metrics & More | Article Recommendations | Supporting Information

ABSTRACT: Microtubules, a major component of the cytoskeleton consisting of tubulin dimers, are involved in various cellular functions, including forming axons and dendrites of neurons and retaining cell shapes by forming various accumulated superstructures such as bundles and doublets. Moreover, microtubule-accumulated structures like swarming microtubule assemblies are attractive components for dynamic materials, such as active matter and molecular robots. Thus, dynamic control of microtubule superstructures is an important topic. However, implementing stimulus-dependent control of superstructures remains challenging. This challenge can be resolved by developing designer protein approaches. We have previously developed a Tau-derived peptide (TP), which binds to the inner or outer surface of microtubules depending on the timing of the incubation. In this report, we designed the TP-fused photoswitchable protein Dronpa (TP-Dronpa) that reversibly photoconverts between monomeric and tetrameric states to photocontrol microtubule assemblies. The formation of microtubule superstructures, including bundles and doublets, was induced by tetrameric TP-Dronpa, whereas monomeric TP-Dronpa ensured that microtubules remained dispersed. Tetrameric TP-Dronpa also induced motile aster-like structures and swarming movement of microtubules on a kinesin-coated substrate. The formation/dissociation of these microtubule superstructures can be controlled by light irradiation. This system can generate and photocontrol various microtubule superstructures and provides an approach to facilitate the assembly of dynamic materials for various applications.

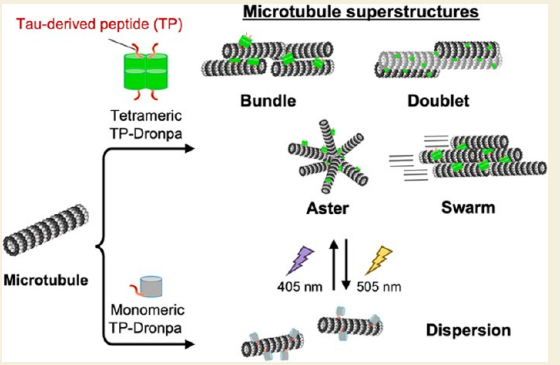

KEYWORDS: *microtubules, Tau-derived peptide, Dronpa, active matter, photoresponsive materials*

INTRODUCTION

Microtubules are tubular cytoskeletons with micrometer lengths and a 15 nm inner diameter that form by polymerizing tubulin dimers with GTP and are involved in various functions, including cell division, cell shape regulation and cell migration.[1−4] In nature, microtubule superstructures are formed by microtubules assembling to form bundles, doublet and aster-like structures. In neurons, microtubule-associated proteins (MAPs), such as Tau and MAP2, bundle microtubules by cross-linking microtubules to contribute to forming axons and dendrites.[5] Microtubules also form doublet structures, which connect a complete microtubule to an incomplete microtubule in flagella and cilia to tolerate physical stresses such as waiving motion.[6−8] Microtubules and associated superstructures play crucial roles as scaffolds of motor proteins such as kinesin and dynein for cargo delivery and the beating of flagella and cilia.[9] The motile properties of microtubules are attracting attention for the construction of active matter and molecular robots.[10−13] In particular, control of microtubule superstructures by external stimuli should facilitate the development of intelligent, active matter.[14] For example, Kakugo et al. achieved optical control of a microtubule swarming motion by conjugating photochromic azobenzene-conjugated complementary DNA to the outer surface of microtubules.[15−17] Moreover, Dogic et al. succeeded in the optical control of forming active gels consisting of microtubules and kinesin-fused iLID, a photoresponsive protein.[18] In nature, regulating axon, dendrite and nucleus formation is conducted by various MAPs that cross-link microtubules.[5] Mimicking the natural system would be useful for controlling microtubule superstructures. However, artificially designed proteins have not been reported for this purpose.

We have previously designed a Tau-derived peptide (TP: CGGGKKHVPGGGSVQIVYKPVDL) based on the repeat domain of Tau, which binds to the inner pocket of microtubules.[19] TP binds to the inner surface of microtubules

Received: October 28, 2024
Revised: January 11, 2025
Accepted: January 13, 2025
Published: January 23, 2025

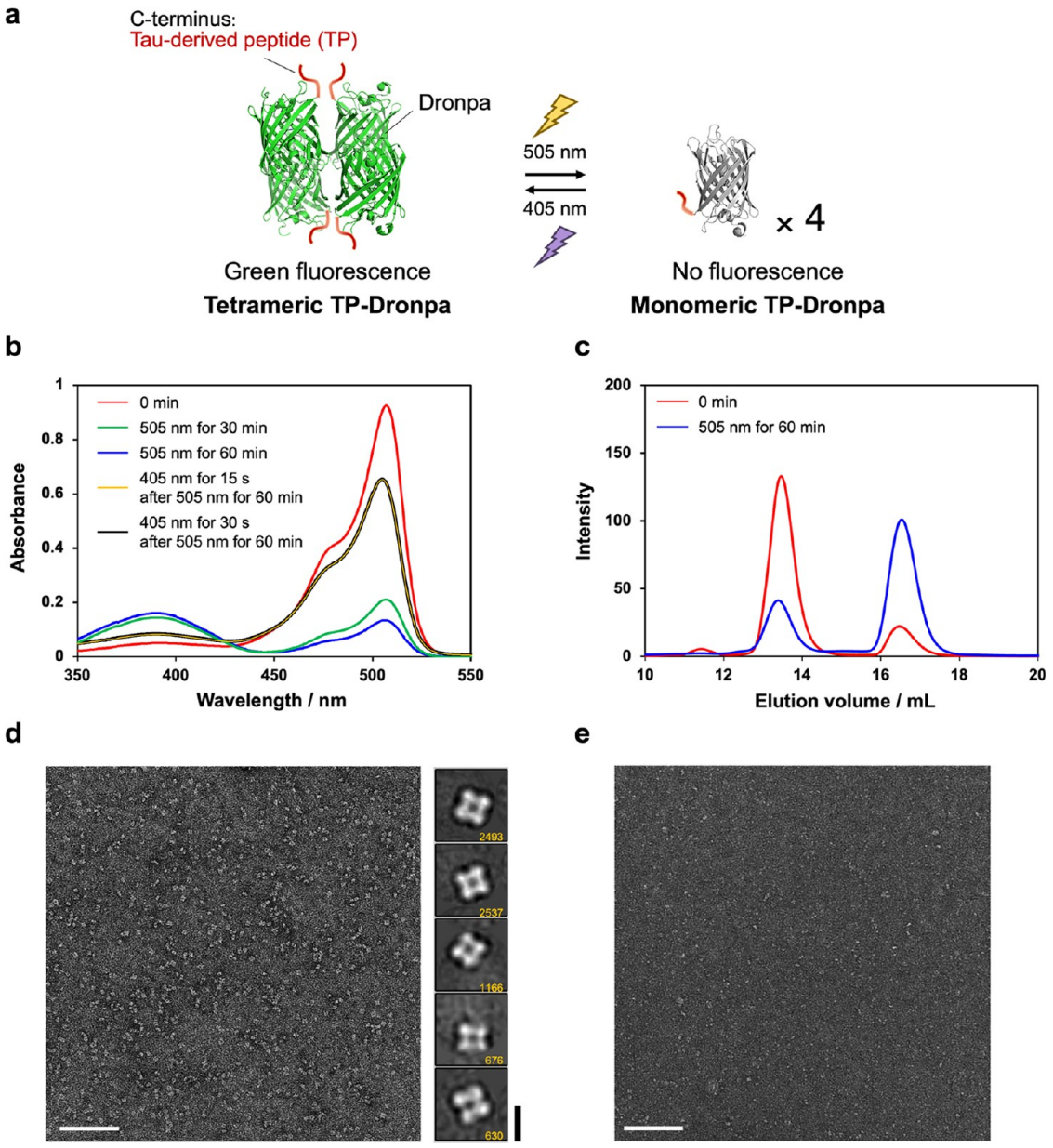

Figure 1. (a) Photoconversion of the association state of Tau-derived peptide (TP)-fused Dronpa (TP-Dronpa). (b) Light irradiation-dependent changes in TP-Dronpa absorbance. The UV−vis spectra of the initial state (red), with 505 nm light irradiation for 30 min (green) or 60 min (blue), 405 nm light irradiation for 15 s (yellow) or 30 s (black) after 505 nm light irradiation for 60 min at 25 °C. Preparation concentration: 11.3 μM TP-Dronpa. Concentrations of TP-Dronpa are defined as the monomer concentrations. (c) Size exclusion chromatography (SEC) analysis of TP-Dronpa. The initial state of TP-Dronpa (red) and after 505 nm irradiation for 60 min (blue). (d and e) Negative staining transmission electron microscopy (TEM) images of a tetrameric fraction of TP-Dronpa (d, left) and a monomeric fraction of TP-Dronpa (e). Class averages of TP-Dronpa showing clear tetrameric structures by single particle analysis ((d), right). The number of particles is indicated in each image. Scale bars, 100 nm for (d) (left) and (e), 10 nm for (d) (right).

by preincubation with tubulin and subsequent microtubule polymerization, whereas TP binds to the outer surface of microtubules by incubation with polymerized microtubules.[19,20] Conjugation of photoreactive molecules, diazirine[21] and spiropyran/merocianine[22] to TP enabled optical control of microtubule stability. However, these small molecule-based approaches do not generate and control the microtubule superstructures. In contrast, the generation of microtubule superstructures, such as bundles and doublets, was observed by binding of TP-fused tetrameric fluorescence protein, Azami-Green (TP-AG), to the outer surface of microtubules.[23] Bundle structures were formed by cross-linking of microtubules by tetrameric TP-AG, and doublet microtubules were formed by recruiting free tubulin to the TP moiety of TP-AG-bound microtubules. Although TP-AG is useful for generating microtubule superstructures, the reversible control of the formation and dissociation of the microtubule superstructures by external stimuli has not yet been achieved. The study of TP-AG inspired us to hypothesize that a photoswitchable tetrameric protein that converts reversibly between monomeric and tetrameric states by light irradiation can photocontrol microtubule superstructures.

In this report, we focused on a photoswitchable protein, Dronpa, which was developed by Miyawaki et al.,[24,25] for

https://doi.org/10.1021/jacsau.4c01017
JACS Au 2025, 5, 791−801

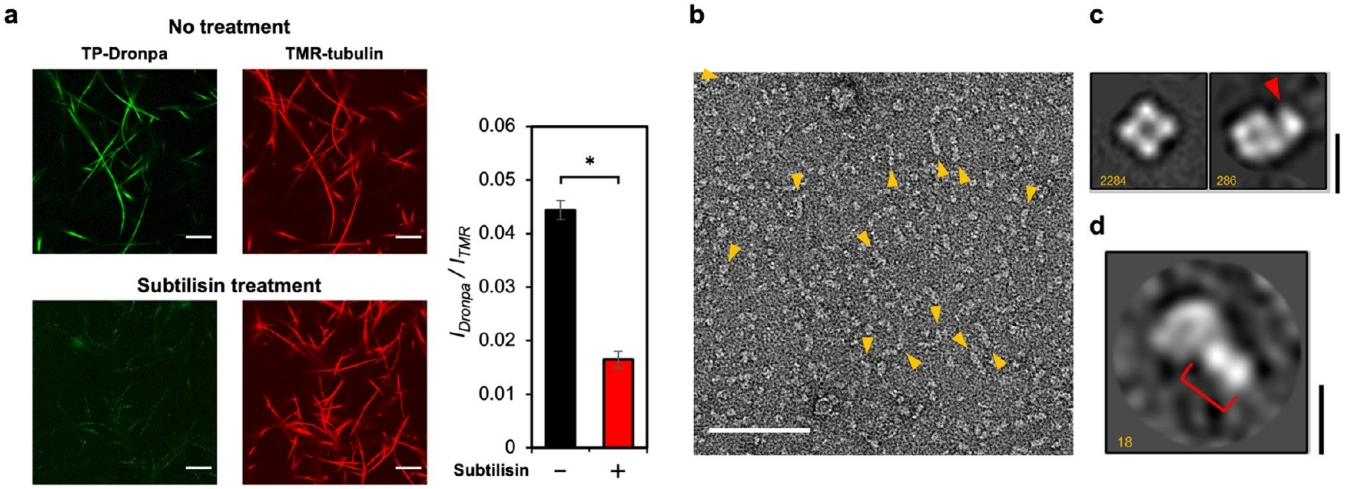

Figure 2. (a) Confocal laser scanning microscopy (CLSM) images of tetrameric TP-Dronpa-incorporated microtubules using intact (top panel) or subtilisin-treated tubulin (bottom panel). Preparation concentrations: 16 μM tubulin, 4 μM TMR-tubulin and 10 μM TP-Dronpa. Scale bars, 10 μm. The I_{Dronpa}/I_{TMR} ratio for each microtubule sample was determined from the CLSM images (right). Error bars represent the standard error of the mean (N = 25). *P < 0.0001, two-tailed Student's t test. (b–d) Analysis of the tetrameric TP-Dronpa-tubulin complex by negative staining TEM. (b) A typical micrograph of tetrameric TP-Dronpa incubated with tubulin. Clear interactions are indicated by the orange arrowheads, with tubulin extending from TP-Dronpa to form filamentous polymers. Preparation concentrations: 20 μM tubulin and 20 μM TP-Dronpa. Scale bar, 100 nm. (c, d) Single particle analysis of tetrameric TP-Dronpa in the presence of tubulin. (c) Typical 2D class averages without (left) and with (right) additional density (red arrowhead) after autopicking. (d) A 2D class average of tetrameric TP-Dronpa binding to tubulin after manual picking. The number of particles is indicated in each image. Scale bar, 10 nm. The red bracket indicates 8 nm additional density.

optical control of microtubule accumulation and dispersion. Tetrameric Dronpa fluoresces green and converts to the monomeric state upon irradiation at 500 nm. In contrast, monomeric Dronpa has no fluorescence and converts to the tetrameric state by 400 nm light irradiation (Figure 1a). Dronpa was used for various applications, including photocontrol of protein localization and accumulation in cells[26,27] and photoreversible protein hydrogels.[28,29] However, there were no attempts to use Dronpa for photocontrolling microtubule assembling structures. In this study, we used the photoswitching of Dronpa for optical control of microtubule assemblies by constructing TP-fused Dronpa construct on its C-terminus (TP-Dronpa). Tetrameric TP-Dronpa facilitated the accumulation of microtubules by cross-linking microtubules with each other, whereas monomeric TP-Dronpa dispersed the microtubule superstructures. Optical control of microtubule superstructures was achieved by switching between the monomeric and tetrameric states of TP-Dronpa.

RESULTS

Design and Binding Analysis of TP-Dronpa to Microtubules

We designed the TP-Dronpa construct containing the Dronpa145N sequence,[30] a Dronpa mutant with the K145N mutation, fused with an N-terminal His-tag and C-terminal TP (Figure S1). This construct was used because the previously designed TP-AG with the same positions of the His-tag and TP generated microtubule superstructures.[23] The plasmid construct was transformed into *E. coli* BL21 and expressed TP-Dronpa was purified by Ni-NTA affinity chromatography (Figure S2). Dronpa without the TP moiety and TP-fused pdDronpa1.2 (TP-pdDronpa) that switches dimeric and monomeric states by light irradiation[31] were prepared using the same construction approach (Figure S2). UV–vis spectra of TP-Dronpa were recorded to evaluate the conversion of the tetrameric/monomeric states by light irradiation (Figure 1a). The initial state of TP-Dronpa was tetrameric, as defined by the prominent peak at 507 nm and a weak peak at 388 nm, as reported previously (Figure 1b).[24] Most of the tetrameric state was converted to the monomeric state by irradiating with 505 nm light (130 mW/cm^2) for 60 min, as observed by an increase in absorption around 400 nm and a decrease in absorption around 500 nm. The temperature of TP-Dronpa solution remained constant during irradiation with 505 nm light for 60 min, indicating that the photothermal effect under these conditions is negligible (Figure S3). Conversely, most monomeric TP-Dronpa converted to the tetrameric state by 405 nm light (113 mW/cm^2) irradiation for 30 s (Figure 1b). The reversibility of the photoconversion of TP-Dronpa between the tetrameric and monomeric states was evaluated by monitoring the absorbance at 507 nm derived from tetrameric TP-Dronpa (Figure S4). The photoconversion of TP-Dronpa was reversible and 40% of the TP-Dronpa population was still able to convert into the tetrameric state even after 7 cycles of photoconversion. These results align with the reported photoresponsivity of Dronpa.[24,25] During the photoconversion process of Dronpa, the tetrameric state is more stable than the monomeric state, thereby requiring much less photon energy for the conversion from monomeric to tetrameric state compared to the reverse process.[24,25] Size exclusion chromatography (SEC) results also showed that TP-Dronpa is converted from tetramer to monomer by 505 nm light irradiation, with an elution shift from 13.5 to 16.5 mL (Figure 1c). The initial state of TP-pdDronpa, which forms a dimer, gave rise to an SEC peak with an elution volume of 14.9 mL (Figure S5), indicating that the peaks of TP-Dronpa at 13.5 and 16.5 mL are tetramer and monomer states, respectively. The existence ratio of TP-Dronpa tetramers and monomers was calculated using the SEC peak areas. For the initial state, 85% of TP-Dronpa formed the tetramer, and 15% of TP-Dronpa formed the monomer. After light irradiation at 505 nm for 60 min, 30% of TP-Dronpa was tetrameric, and

https://doi.org/10.1021/jacsau.4c01017
JACS Au 2025, 5, 791–801

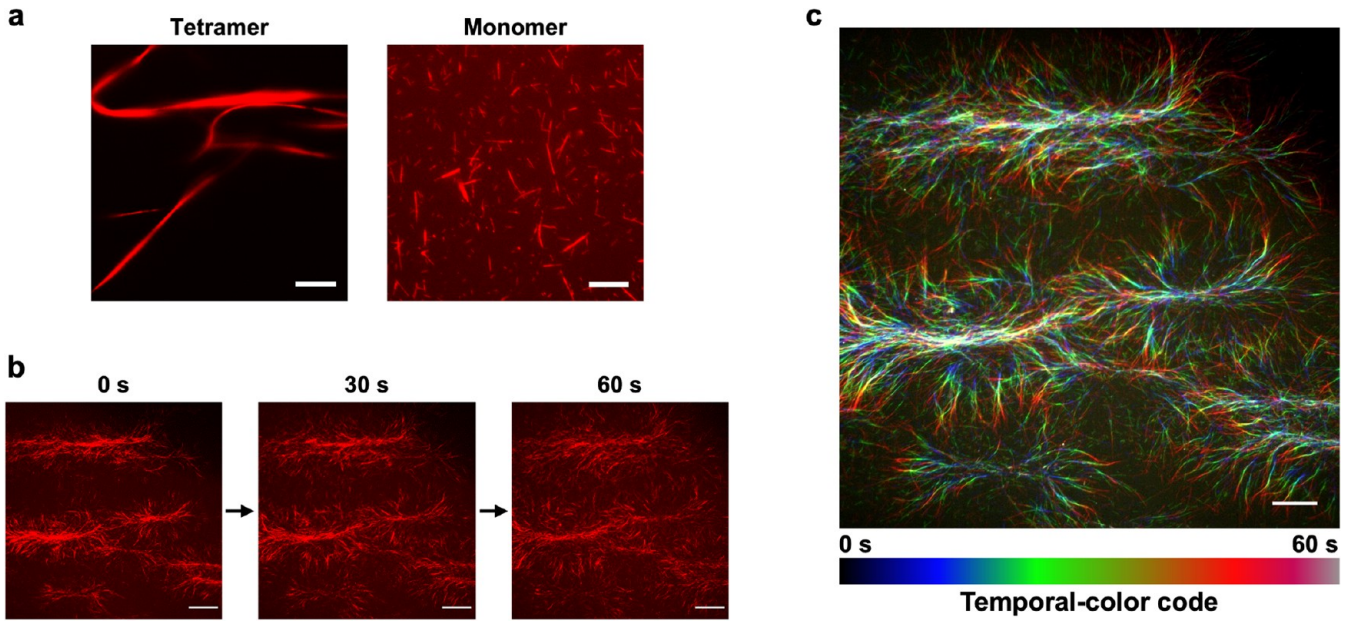

Figure 3. (a) CLSM images of microtubules incorporated with tetrameric TP-Dronpa or monomeric TP-Dronpa. Preparation concentrations: 16 μM tubulin, 4 μM TMR-tubulin and 10 μM TP-Dronpa. Scale bars, 10 μm. (b) Time-lapse images showing the dissociation of bundled microtubules incorporated with tetrameric TP-Dronpa into aster-like structures on the kinesin-coated substrate. Scale bars, 30 μm. (c) A fluorescence microscopy image of moving aster structures in Figure 3b using a temporal-color code. The time series images were color-coded and superimposed to visualize the movement of microtubules. The color scales are shown at the bottom of the image. Scale bar, 20 μm.

70% of TP-Dronpa was monomeric. The 13.5 and 16.5 mL peak fractions were negatively stained and observed by transmission electron microscopy (TEM). The 13.5 mL peak fraction sample showed unambiguous tetrameric structures with diameters of ∼10 nm, which was also confirmed by single particle analysis (Figure 1d). In contrast, the 16.5 mL peak fraction sample showed smaller particles with ∼5 nm diameters corresponding to the TP-Dronpa monomer (Figure 1e).

Next, the binding of tetrameric TP-Dronpa to microtubules was evaluated by confocal laser scanning microscopy (CLSM). Tetramethylrhodamine (TMR)-labeled tubulin was polymerized by guanosine-5′-[(α,β)-methyleno]triphosphate (GMPCPP), a GTP analog used to form stable microtubules. TP-Dronpa was incubated with the TMR-labeled microtubules, and CLSM was performed. Co-localization of TMR and Dronpa fluorescence on microtubules was observed (Figure 2a, top left), indicating that TP-Dronpa bound to microtubules. In contrast, tetrameric Dronpa without the TP moiety showed weaker binding to microtubules than TP-Dronpa (Figure S6), indicating that the TP sequence is essential for microtubule binding by TP-Dronpa. Additionally, the binding of dimeric TP-pdDronpa to microtubules was weak (Figure S7). These results indicate that the differences between TP-Dronpa and TP-pdDronpa, such as the number of TPs, size and surface charge (TP-Dronpa has a more negative charge than TP-pdDronpa), affect microtubule binding. The binding site of TP-Dronpa to microtubules was then estimated using subtilisin, an enzyme that selectively digests the C-terminal tails of tubulin located on the outer surface of microtubules.[23,32] When the microtubules were prepared using subtilisin-treated tubulin, the fluorescence of tetrameric TP-Dronpa localized on the microtubules decreased dramatically (Figure 2a, bottom left). This result indicates that TP-Dronpa mainly binds to the C-terminus of tubulin, the outer surface of microtubules. The binding property of monomeric and tetrameric TP-Dronpa to microtubules was evaluated by a co-sedimentation assay (Figure S8). Free TP-Dronpa and TP-Dronpa bound to microtubules were separated by ultracentrifugation and quantified by SDS-PAGE.[23] The binding ratio of TP-Dronpa to microtubules estimated in this assay showed that the binding affinity of tetrameric TP-Dronpa to microtubules (K_d = 9.7 μM) was stronger than that of monomeric TP-Dronpa (K_d = 51 μM), possibly because of multivalent binding. The binding affinity of tetrameric TP-Dronpa was similar to the previously reported affinity of TP-AG to microtubules (K_d = 11 μM).[23] Additionally, the TP-Dronpa-tubulin complex was observed by TEM by incubating TP-Dronpa with tubulin (Figure 2b–d). This result indicates that TP-Dronpa binds to tubulin and microtubules. Because the recruitment of tubulin to TP-AG on microtubules is important for generating microtubule superstructures,[23] tubulin binding to TP-Dronpa should aid the construction of superstructures.

Microtubule Accumulation Induced by TP-Dronpa

We next evaluated the effect of TP-Dronpa on the motility of microtubules driven by ATP hydrolysis on a kinesin-coated glass substrate (motility assay). Before adding ATP, the microtubules with tetrameric TP-Dronpa appeared as thick bundle structures, whereas the microtubules with monomeric TP-Dronpa were separated and not bundled (Figure 3a). These results indicate tetrameric TP-Dronpa tethered microtubules by the four TPs exposed on the Dronpa scaffold, whereas cross-linking by monomeric TP-Dronpa to microtubules was not observed. The concentration dependence of TP-Dronpa showed that 0.5 equiv of TP-Dronpa to tubulin was sufficient to induce the formation of the bundled microtubules (Figure S9). Adding ATP to microtubule bundles with tetrameric TP-Dronpa induced conversion into radially moving aster-like structures and subsequent dissociation (Figure 3b,c and Movie S1). In contrast, microtubules with

https://doi.org/10.1021/jacsau.4c01017
JACS Au 2025, 5, 791−801

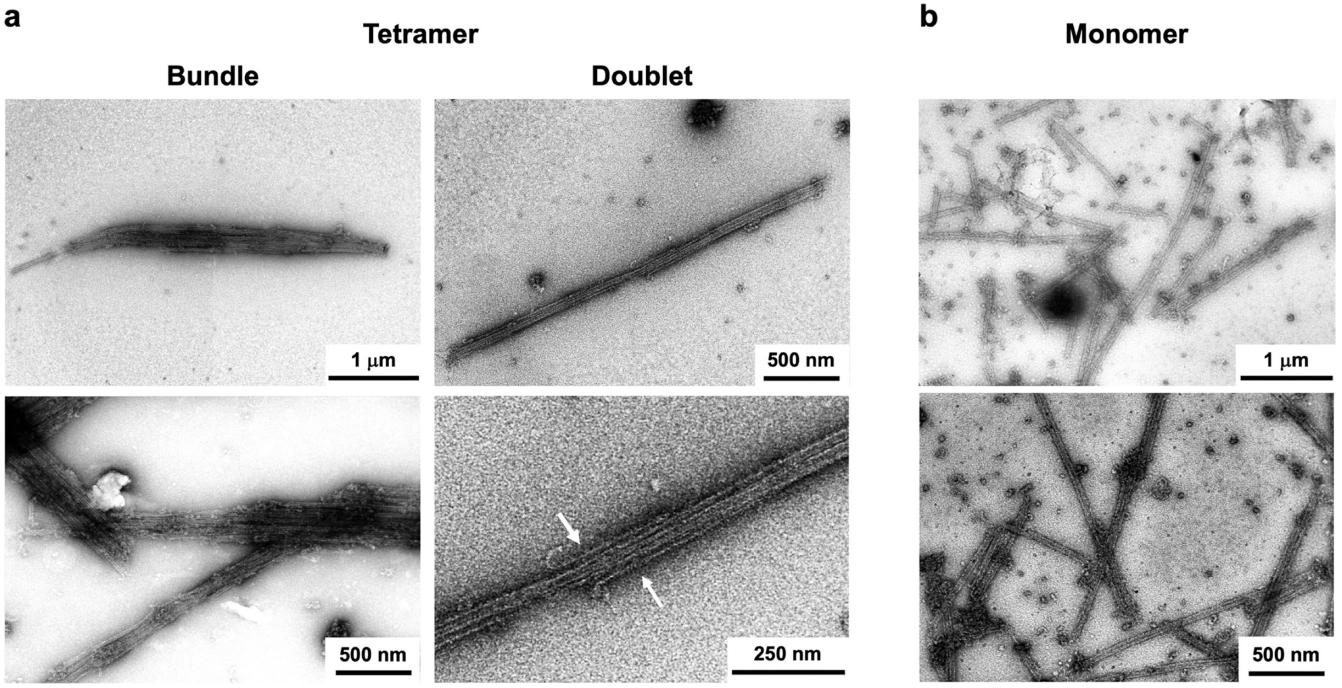

Figure 4. TEM images of TP-Dronpa-incorporated microtubules. Preparation concentrations: 16 μM tubulin, 4 μM TMR-tubulin and 10 μM TP-Dronpa. (a) Bundled microtubules (left) and doublet microtubules (right) bound with tetrameric TP-Dronpa. Additional layers of microtubules were observed (white arrow). (b) Dispersed microtubules bound with monomeric TP-Dronpa.

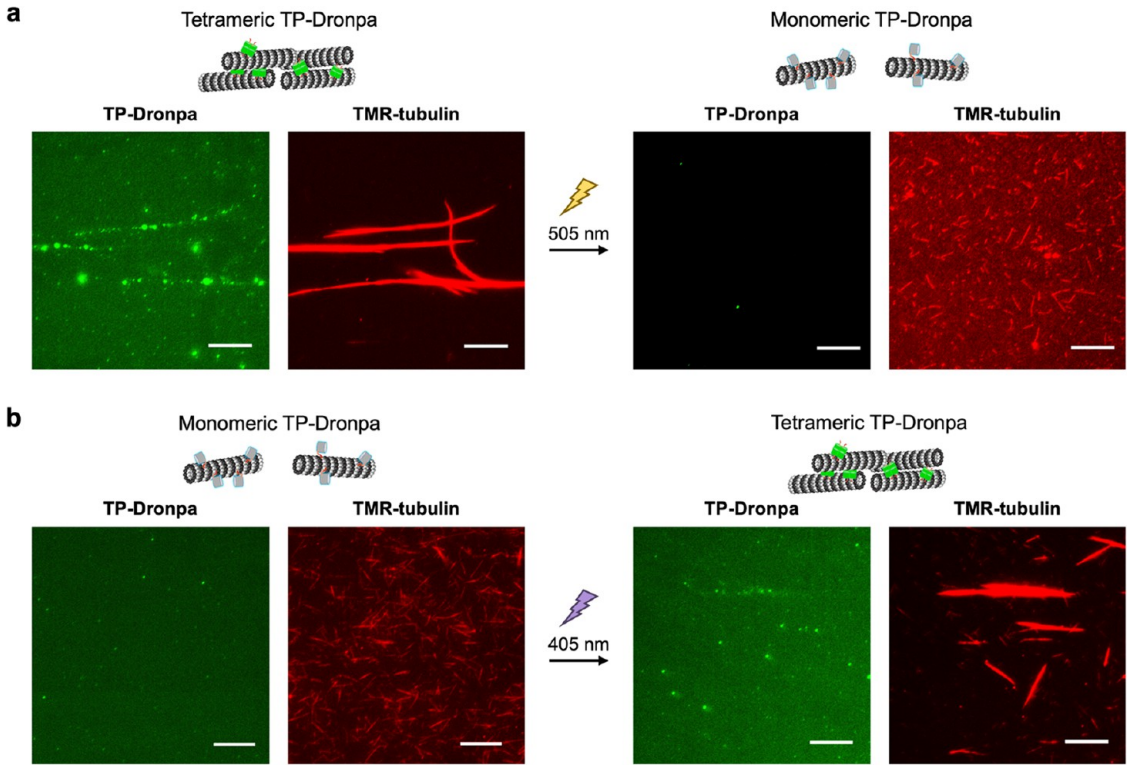

Figure 5. Optical control of microtubule accumulation and dispersion by TP-Dronpa. (a) Dissociation of microtubule assembly by 505 nm light irradiation for 60 min to microtubules incorporated with tetrameric TP-Dronpa. (b) Accumulation of microtubules by 405 nm light irradiation for 30 s to microtubules incorporated with monomeric TP-Dronpa. Preparation concentrations: 16 μM tubulin, 4 μM TMR-tubulin and 10 μM TP-Dronpa. Scale bars, 10 μm.

monomeric TP-Dronpa moved individually like normal microtubules (Movie S2). The conversion of the bundles into aster-like structures may be caused by the random association of microtubule bundles with tetrameric TP-Dronpa in a parallel and antiparallel manner, followed by dissociation such as asters by the moving of kinesin. These results showed completely different microtubule assembly structures by tetrameric and monomeric TP-Dronpa.

https://doi.org/10.1021/jacsau.4c01017
JACS Au 2025, 5, 791−801

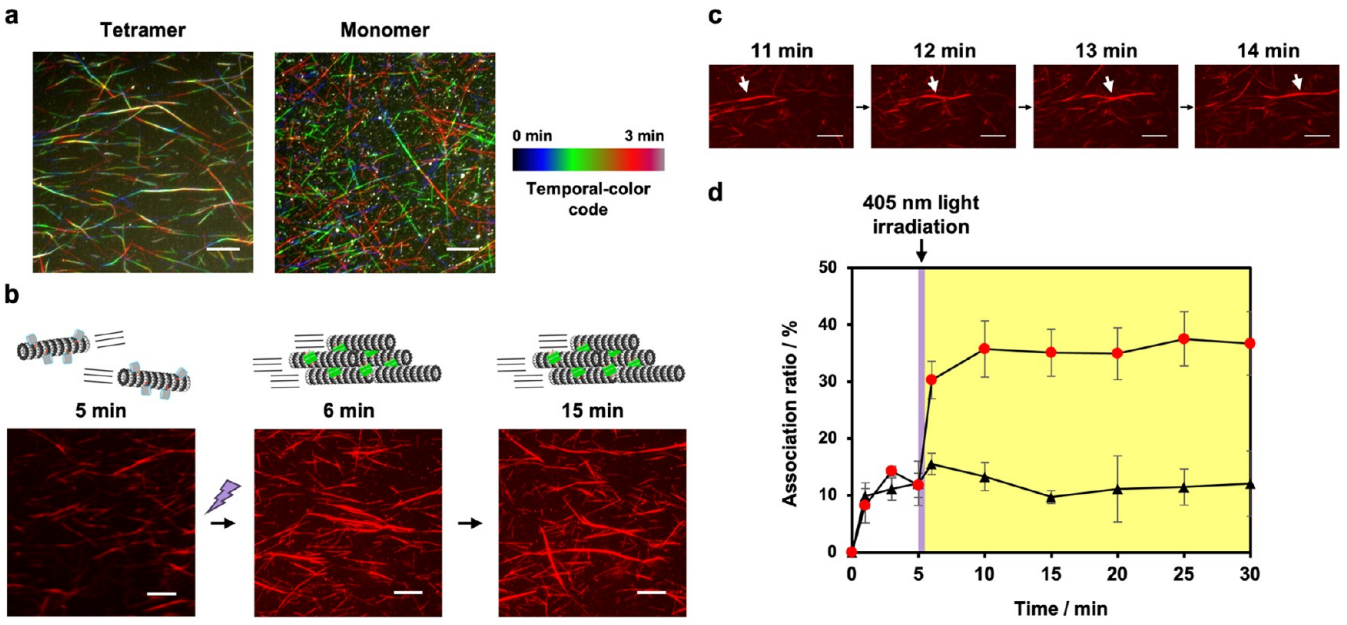

Figure 6. Photocontrol of motile TP-Dronpa-incorporated microtubule assembly under depleting conditions. (a) Fluorescence microscopy images of microtubules incorporated with tetrameric TP-Dronpa or monomeric TP-Dronpa on a kinesin substrate in the presence of 0.2% methylcellulose. Preparation concentrations: 16 μM tubulin, 4 μM TMR-tubulin and 10 μM TP-Dronpa. Scale bars, 10 μm. (b) Time-lapse images showing the accumulation of monomeric TP-Dronpa-incorporated microtubules by 405 nm light irradiation for 30 s at 5 min. Preparation concentrations: 1 μM tubulin, 1 μM TMR-tubulin and 5 μM TP-Dronpa. Scale bars, 10 μm. (c) Representative time-lapse fluorescence microscopy images showing the formation of a bundled microtubule. Scale bars, 10 μm. (d) Change of the association ratio of microtubules over time with 405 nm light irradiation for 30 s at 5 min (red dot) and without light irradiation (black triangle). Error bars represent the standard deviation of the mean (N = 3).

TEM Observation of Microtubule Superstructures

TP-Dronpa-incorporated microtubule structures were observed by TEM. Initially, bundled microtubules with around 200 nm widths were observed by treatment with tetrameric TP-Dronpa (Figure 4a, left). In addition to bundled structures and normal singlet microtubules with 25 nm diameter, doublet-like microtubules consisting of two microtubules with 25 nm (A-tubules) and 15 nm (B-tubules) diameters, typically observed in flagella and cilia,[8] were observed (Figures 4a, right and S10). The formation of doublet microtubules has been observed previously by treatment of tetrameric TP-AG.[23] Similar to TP-AG, tetrameric TP-Dronpa bound to the outer surface of microtubules and recruited free tubulin by binding the TP moiety of TP-Dronpa (Figure 2d) to induce the formation of doublet microtubules. In contrast, bundled and doublet microtubules were not observed for monomeric TP-Dronpa (Figure 4b). These results indicate that tetrameric TP-Dronpa induced the formation of microtubule bundles and doublet structures, whereas monomeric TP-Dronpa showed no such effects, supporting the fluorescent microscopy results (Figure 3a).

Optical Control of Microtubule Accumulation and Dispersion

Optical control of microtubule accumulation and dispersion was demonstrated by converting monomeric and tetrameric states of TP-Dronpa. Tetrameric TP-Dronpa-incorporated microtubules were prepared, and irradiation with 505 nm light for 60 min was performed to convert tetrameric TP-Dronpa to the monomeric state. Light irradiation converted the bundled microtubules into dissociated and dispersed microtubules (Figure 5a). The fluorescence of tetrameric TP-Dronpa on the microtubules was also observed to decrease following 505 nm light irradiation, indicating the conversion of tetrameric TP-Dronpa to the monomer state. The dispersed microtubules moved individually on the kinesin substrate, as seen for normal microtubules (Movie S3). When monomeric TP-Dronpa-incorporated microtubules were irradiated with 405 nm light for 30 s to convert TP-Dronpa from the monomeric to tetrameric state, the dispersed microtubules accumulated into bundles, with partial recovery of the fluorescence of tetrameric TP-Dronpa (Figure 5b). These bundled microtubules converted aster-like structures and dissociated by the moving of kinesin (Movie S4), as observed in the microtubules with tetrameric TP-Dronpa (Figure 3). These results indicate that microtubule accumulating structures were modulated by the photoconverting tetrameric and monomeric states of TP-Dronpa. The photoconversion ratio of monomeric TP-Dronpa bound to microtubules into the tetrameric state was estimated by the fluorescence intensity from tetrameric TP-Dronpa by comparing before and after 405 nm light irradiation and after removal of free TP-Dronpa from solutions by ultracentrifugation (Figure S11). The result showed that ∼18% of monomeric TP-Dronpa bound to microtubules was converted to the tetrameric state by 405 nm light irradiation. Thus, the photocontrol of microtubule accumulating structures was achieved by reversible conversion of the monomeric and tetrameric states of TP-Dronpa on microtubules.

Optical Control of Microtubule Swarming

To achieve temporal accumulation and "swarming" movement of microtubules by TP-Dronpa, we used methylcellulose, which is frequently used as a depletion agent to promote the association of microtubules in the motility assay.[33] Under depleting conditions using methylcellulose, microtubule accumulation and swarming movement in a parallel direction are promoted. In our system, methylcellulose was used to

https://doi.org/10.1021/jacsau.4c01017
JACS Au 2025, 5, 791−801

increase the affinity of TP-Dronpa to microtubules during the motility assay for optical control of microtubule accumulation and swarming. When tetrameric TP-Dronpa, ATP and 0.2% methylcellulose were added to microtubules fixed on the kinesin substrate, accumulation of microtubules and swarming movement were observed (Figure 6a, Movie S5). Under these conditions, tetrameric TP-Dronpa possibly cross-linked microtubules, which moved in the same direction to form the accumulated structures in parallel. In contrast, microtubules moved individually using monomeric TP-Dronpa (Figure 6a, Movie S5). The velocity of these microtubules was 0.20 ± 0.009 μm/s for the monomeric TP-Dronpa-incorporated microtubules and 0.077 ± 0.020 μm/s for the tetrameric TP-Dronpa-incorporated microtubules (Figure S12). The reduced velocity of microtubules with tetrameric TP-Dronpa may arise from the suppression of microtubule movement because of induced antiparallel cross-linking of moving microtubules by a fraction of tetrameric TP-Dronpa.

Accumulation and swarming of microtubules were observed by treating tetrameric TP-Dronpa, whereas monomeric TP-Dronpa showed no such effect (Figure 6a), and therefore temporal optical control of microtubule accumulation was attempted. The movement of microtubules with monomeric TP-Dronpa was observed for 5 min, and then the sample was irradiated at 405 nm for 30 s to convert the monomeric form to the tetrameric state. Irradiation at 405 nm induced the accumulation of microtubules and swarming movement (Figure 6b,c, Movie S6). The association ratio of microtubules increased drastically after 405 nm light irradiation (Figure 6d). The photoconverted tetrameric TP-Dronpa on microtubules probably cross-linked microtubules in a parallel manner. These results show the optical control of microtubule accumulation and swarming by conversion of monomeric and tetrameric states of TP-Dronpa bound with microtubules.

DISCUSSION

In this report, control of accumulation and dispersion of microtubules was achieved by photoconverting the monomeric/tetrameric states of TP-Dronpa. Modifying photoresponsive DNAs to microtubules was used previously to control the accumulation/dispersion of microtubules by light irradiation.[15−17] However, this system required direct conjugation of DNA to microtubules and could not be used to control intact microtubules. Moreover, the accumulated structures were restricted to swarming microtubules. In this study, various microtubule superstructures were generated and photocontrolled by TP-Dronpa without directly modifying microtubules. Interestingly, random accumulation (parallel and antiparallel) of microtubules and conversion to aster-like structures were observed by tetrameric TP-Dronpa, whereas swarming microtubules in a parallel direction were generated on a kinesin substrate with depletion force. In addition, our system uses a fluorescence switchable protein that will facilitate tracking microtubule accumulation and dispersion by fluorescent imaging. Moreover, this protein-based accumulation/dispersion system can be used to model natural systems forming microtubule superstructures.

CONCLUSIONS

Optical control of microtubule accumulation and dispersion was achieved by Tau-derived peptide-fused photoswitchable Dronpa. TP-Dronpa bound to the outer surface of microtubules and formed bundling, doublet and aster-like microtubule superstructures in the tetrameric state. Optical control of these microtubule superstructures was achieved by photoconversion between the monomeric and tetrameric states of TP-Dronpa. This work demonstrates protein-based optical control of intact microtubules mimicking the formation of microtubule superstructures in nature. In the future, the TP-Dronpa system, a genetically encodable protein system, will be applied to manipulate cell shape and migration direction by optical control of intracellular microtubule accumulation and will be used in nanomaterial research, such as the development of active matter and molecular robotics.

MATERIALS AND METHODS

Construction of Plasmids

The TP-Dronpa, Dronpa, and TP-pdDronpa expression vectors were constructed based on the pET-29b(+) expression vector (Merck, Darmstadt, Germany). The TP-Dronpa, Dronpa, and TP-pdDronpa genes were synthesized to optimize codon usage for *Escherichia coli*. The open circular pET-29b(+) vector was synthesized by inverse polymerase chain reaction (PCR). PCR was performed in the TaKaRa PCR Thermal Cycler Dice Touch (TaKaRa) using the Tks Gflex DNA Polymerase (TaKaRa). The synthetic genes coding TP-Dronpa, Dronpa, and TP-pdDronpa were ligated into the open circular pET-29b(+) using the In-Fusion HD Cloning Kit (TaKaRa) to generate the recombinant protein expression vectors. The plasmids were sequenced by Eurofins Genomics.

Expression and Purification of Proteins

The pET-29b(+) vectors coding TP-Dronpa, Dronpa, and TP-pdDronpa were transformed into *E. coli* ClearColi BL21(DE3) strain (Biosearch Technologies) by a heat-shock procedure. Bacterial cells were spread on Luria−Bertani−Ampicillin (LBA) (100 μg/mL) agar and grown overnight at 37 °C. A single transformant colony was grown in LBA medium at 37 °C overnight. The culture was diluted 100-fold by addition to fresh LBA medium and grown at 37 °C until an absorbance of 0.5 reached at 600 nm (mid logarithmic phase). Then, the culture was incubated with 0.1 mM isopropyl β-D-1-thiogalactopyranoside at 20 °C. After 18 h of incubation, cells were harvested by centrifugation at 8,000 rpm for 10 min. The cell pellets were suspended in Ni-affinity binding buffer [50 mM tris-HCl (pH 7.4), 150 mM NaCl, and 20 mM imidazole] on ice. The cells were lysed by sonication. After centrifugation at 13,000 rpm for 10 min, the supernatant was loaded onto 1 mL of Ni-affinity column (Cytiva). After washing with the same buffer and the storage buffer [50 mM tris-HCl (pH 8.0) and 300 mM NaCl], the protein was eluted from the column using the Ni-affinity elution buffer [50 mM tris-HCl (pH 8.0), 300 mM NaCl, and 250 mM imidazole]. The eluted sample was dialyzed against the storage buffer [Spectra/por7; cutoff molecular weight (Mw), 8 kDa; Spectrum Laboratories Inc.] at 4 °C. The purity of proteins was evaluated by SDS-PAGE (Figure S2). The concentration of proteins was determined using reported molar extinction coefficients.[24]

UV−vis Spectrum Measurement

LED light (CL-1503 or CL-1501, ASAHI SPECTRA, 405 nm: 113 mW/cm^2 or 505 nm: 130 mW/cm^2) was irradiated to the solution of 11.3 μM TP-Dronpa in the storage buffer with 505 nm light for 30 or 60 min at a distance of 9 cm from bottom of Eppendorf tube, and then UV−vis spectra were measured at 25 °C. After that, 405 nm light was irradiated to the solution of TP-Dronpa, and then UV−vis spectra were measured at 25 °C. Temperature of the Eppendorf tube containing the 11.3 μM TP-Dronpa solution in the storage buffer during irradiation of 505 nm light for 60 min was monitored using a thermocouple thermometer (MC1000-000, Chino Corp.). To analyze the reversible photoconversion of TP-Dronpa between the tetrameric and monomeric states, 60 μM TP-Dronpa in the storage buffer was irradiated with 505 nm light for 60 min, followed by 405 nm light for

https://doi.org/10.1021/jacsau.4c01017
JACS Au 2025, 5, 791−801

30 s. The cycle was repeated and the absorbance at 507 nm derived from tetrameric TP-Dronpa was measured in each step using NanoDrop One[c] (Thermo Fisher Scientific).

SEC Analysis

For TP-Dronpa, the protein sample purified by Ni-NTA purification (8.7 mg/mL) was diluted 5-fold with the storage buffer, achieving a final volume of 500 μL. Then the samples with or without radiation with a 505 nm light (CL-1501, ASAHI SPECTRA) were ultracentrifuged (25,000 rpm for 20 min, himac S55A2 rotor), and then applied to a Superdex 200 Increase 10/300 GL column (Cytiva) equilibrated with the storage buffer. For TP-pdDronpa protein, 9.5 mg/mL protein sample after Ni-NTA purification was ultracentrifuged (25,000 rpm for 20 min, himac S55A2 rotor), and then applied to a Superdex 200 Increase 10/300 GL column (Cytiva) equilibrated with the storage buffer. The fractions with target proteins were collected and pooled.

Binding Analysis of TP-Dronpa to Microtubules

C-terminal tails of tubulin were removed by the treatment of subtilisin according to the reported procedure with modification.[32] Mixture of tubulin (192 μM) and TMR-tubulin (48 μM) in BRB80 [80 mM PIPES (pH 6.9), 1.0 mM $MgCl_2$, and 1.0 mM EGTA] were treated with subtilisin in a subtilisin:tubulin ratio of 1:500 (w/w) at 4 °C for 30 min. Then, the subtilisin activity was inhibited by incubation with 5 mM phenylmethylsulfonyl fluoride at 4 °C for 10 min. After centrifugation at 21,000 rpm at 4 °C for 20 min, the supernatants were collected and used as subtilisin-treated tubulin. Then, 2 μL of GMPCPP premix (1 mM GMPCPP and 20 mM $MgCl_2$ in BRB80) was added to 8 μL of the solution containing subtilisin-treated tubulin in BRB80. The mixture was incubated at 37 °C for 30 min in the dark. Then 60 μM TP-Dronpa (2 μL) was added to the mixture and kept at 25 °C for 30 min in the dark (final concentrations: [Tubulin] = 19.2 μM, [TMR-tubulin] = 4.8 μM, [TP-Dronpa] = 12 μM, and [GMPCPP] = 0.2 mM). As a control, tubulin without subtilisin treatment was used instead of subtilisin-treated tubulin. Dronpa without TP and TP-pdDronpa were also used for the binding experiments using tubulin without subtilisin treatment. TP-Dronpa and TMR fluorescence intensity per microtubule were measured from the fluorescence images by subtracting the background intensity using ImageJ software. The background-subtracted TP-Dronpa fluorescence intensity and TMR fluorescence intensity for each microtubule (N = 25) were calculated from 5 images to estimate the binding of TP-Dronpa to microtubules.

Co-sedimentation Assay

Tetrameric TP-Dronpa was used in the initial state of purified TP-Dronpa. Monomeric TP-Dronpa was prepared by 505 nm light irradiation (130 mW/cm^2) to tetrameric TP-Dronpa for 60 min at room temperature. GMPCPP premix (6 μL) was mixed with a solution (18 μL) containing tubulin (0, 8.3, 16.7, 33.3, 66.7 μM) in BRB80. The mixture was incubated at 37 °C for 30 min in the dark. Then, tetrameric or monomeric TP-Dronpa (100 μM, 6 μL) was added to the mixture and kept at 25 °C for 30 min in the dark (final concentrations: [Tubulin] = 0, 5, 10, 20, 40 μM, [TP-Dronpa] = 20 μM, and [GMPCPP] = 0.2 mM). After ultracentrifugation of the mixture at 50,000 rpm at 37 °C for 5 min, the supernatants and the pellets were collected and analyzed by SDS-PAGE. The ratio of TP-Dronpa bound to microtubules (θ) was calculated as the ratio of the density of TP-Dronpa bands in the supernatants and the pellets. The results were treated with the following Hill eq (eq 1) to give the dissociation constant (K_d) and the Hill coefficient (n).

$$\log\left(\frac{\theta}{1-\theta}\right) = n \log \frac{1}{K_d} + n \log[\text{Tubulin}] \quad (1)$$

Motility Assay

GMPCPP premix (2 μL) was mixed with a solution (5 μL) containing tubulin (32 μM) and TMR-tubulin (8 μM) in BRB80. The mixture was incubated at 37 °C for 30 min in the dark. Then TP-Dronpa (34 μM, 3 μL, monomer or tetramer prepared as above) was added to the mixture and kept at 25 °C for 30 min in the dark (final concentrations: [Tubulin] = 16 μM, [TMR-tubulin] = 4 μM, [TP-Dronpa] = 10 μM, and [GMPCPP] = 0.2 mM). The samples were diluted 50-fold by BRB80. Flow cells were prepared by making a narrow channel on a 24 mm by 60 mm coverslip covered with an 18 mm by 18 mm coverslip (Matsunami, Osaka, Japan) using double-sided tape as a spacer. First, casein (0.5 mg/mL) in BRB80 was introduced into the flow cells and incubated for 3 min. Then, the solution was exchanged with wash buffer [casein (0.5 mg/mL), D-glucose (4.5 mg/mL), glucose oxidase (50 U/mL), catalase (50 U/mL), 1.0 mM dithiothreitol, and 1.0 mM $MgCl_2$ in BRB80] containing 700 nM kinesin and incubated for 3 min. After washing with wash buffer, the solution was exchanged with microtubule solution and incubated for 3 min. After washing with wash buffer, the solution was exchanged with wash buffer containing 5.0 mM ATP and 1.0 mM Trolox. Then, the motility of microtubules was imaged every 10 s. All the experiments were performed at room temperature.

TEM Observation of TP-Dronpa and TP-Dronpa Incubated with Tubulin

Monomeric and tetrameric TP-Dronpa fractions after SEC were diluted with the storage buffer (final concentration: [TP-Dronpa] = 15 μg/mL) and used for negative staining TEM. For the TP-Dronpa-tubulin complex, tetrameric TP-Dronpa fraction and tubulin were mixed (Final concentrations: [Tubulin] = 20 μM, [TP-Dronpa] = 20 μM) and incubated at 25 °C for 30 min, and the sample was diluted 100 times. Sample solutions (3.5 μL) were applied to carbon-coated Cu-grids (U1013, EM Japan Co., Ltd.) prehydrophilized using PELCO easiGlow (TED PELLA, INC.) and incubated for 3 min and the excess solution was removed. Then, grids were flipped and sequentially touched to two drops of Milli-Q water and two drops of 1.5% uranyl acetate, then put on a drop of 1.5% uranyl acetate for 30 s. The remaining solution on the grids was removed by filter paper and dried at room temperature. After that, samples were imaged in a TEM (Talos L120C TEM, Thermo Fisher Scientific) operating at an accelerating voltage of 120 kV. Images were collected for each sample in a pixel size of 1.548 Å/pixel.

Single Particle Analysis

Obtained TEM images were imported into Relion 3.0. For the tetrameric TP-Dronpa sample, particles were picked automatically using the template-free procedure based on a Laplacian-of-Gaussian (LoG) filter in Relion, yielding a total of 33,114 particles from 60 micrographs, and the particles were extracted in a box size of 128 pixels and underwent reference-free 2D classification using a 200-Å mask, and classified into 100 classes. Typical classes showing clear tetrameric structure are shown in Figure 1d. For the TP-Dronpa-tubulin complex, the particles were first picked automatically using the LoG filter in Relion, yielding 94,112 particles from 161 micrographs. The particles were extracted with a box size of 128 pixels and classified into 100 classes using reference-free 2D classification with a 200-Å mask. Representative class averages are shown in Figure 2c. Subsequently, a manual picking was conducted to enhance the clarity of the results. 228 particles of tetrameric TP-Dronpa with additional densities were picked by visual inspection and then extracted with a box size of 192 pixels. These particles were then further classified by a 2D classification using a 270-Å mask, segmented into five classes. A typical class average is shown in Figure 2d.

TEM Observation of TP-Dronpa-Incorporated Microtubules

Monomeric or tetrameric TP-Dronpa-incorporated microtubules were prepared as above (Final concentrations: [Tubulin] = 16 μM, [TMR-tubulin] = 4 μM, [TP-Dronpa] = 10 μM, [GMPCPP] = 0.2 mM). Sample solution (5 μL) was applied to carbon-coated Cu-grids (Thin Carbon film coated TEM Grids, Science Service) for 1 min and then removed. Then, the 16% EM stainer (Nisshin EM Co., Ltd.) was applied to the TEM grids for 3 min and removed. Then, carbon-coated grids were dried in a desiccator. After that, microtubules were imaged in TEM (JEOL JEM 1400 Plus) at an accelerating voltage of 80 kV.

https://doi.org/10.1021/jacsau.4c01017
JACS Au 2025, 5, 791−801

Optical Control of Accumulation and Dispersion of TP-Dronpa-Incorporated Microtubules

Monomeric or tetrameric TP-Dronpa-incorporated microtubules were prepared as above (Final concentrations: [Tubulin] = 16 μM, [TMR-tubulin] = 4 μM, [TP-Dronpa] = 10 μM, [GMPCPP] = 0.2 mM). To convert tetrameric TP-Dronpa to a monomeric state, 505 nm light (130 mW/cm^2) was irradiated to the tetrameric TP-Dronpa-incorporated microtubules for 60 min at room temperature. To convert monomeric TP-Dronpa to a tetrameric state, 405 nm light (113 mW/cm^2) was irradiated to the monomeric TP-Dronpa-incorporated microtubules for 30 s at room temperature. These samples were diluted 50-fold by BRB80. Flow cells were prepared as above. First, casein (0.5 mg/mL) in BRB80 was introduced into the flow cells and incubated for 3 min. Then, the solution was exchanged with wash buffer [casein (0.5 mg/mL), D-glucose (4.5 mg/mL), glucose oxidase (50 U/mL), catalase (50 U/mL), 1.0 mM dithiothreitol, and 1.0 mM $MgCl_2$ in BRB80] containing 700 nM kinesin and incubated for 3 min. After washing with wash buffer, the solution was exchanged with microtubule solution and incubated for 3 min. After washing with wash buffer, microtubules were imaged by fluorescence microscopy.

Optical Control of Motile TP-Dronpa-Incorporated Microtubule Assembly

Microtubules were prepared as above (Final concentrations: [Tubulin] = 1 μM, [TMR-tubulin] = 1 μM, [GMPCPP] = 0.2 mM). For the conversion of tetrameric TP-Dronpa to a monomeric state, 505 nm light (130 mW/cm^2) was irradiated for 60 min at room temperature. This sample was diluted 2-fold by BRB80. Flow cells were prepared as above. Before imaging by fluorescence microscopy, the solution in the flow cell was exchanged with wash buffer containing 5.0 mM ATP, 1.0 mM Trolox, 0.2% methylcellulose, and 5 μM of tetrameric or monomeric TP-Dronpa. In the case of irradiation of 405 nm light for tetramerization of TP-Dronpa during time-lapse imaging, the solution in the flow cell was exchanged with wash buffer containing 5.0 mM ATP, 1.0 mM Trolox, 0.2% methylcellulose, and 5 μM of monomeric TP-Dronpa before imaging, and the light was irradiated for 30 s on the fluorescence microscope. The association ratio at a given time t was determined by manually counting the number of single microtubules and dividing the number at time t by the number present initially (t = 0). The time-dependent association ratio $R(t)$ of TMR-labeled microtubules was determined as following eq (eq 2) with N_0 = Initial number of single microtubules, N (t) = Number of single microtubules after time t. The mean association ratio was obtained from the average of three regions of interest (73.3 μm × 73.3 μm).

$$R(t) = \frac{N_0 - N(t)}{N_0} \quad (2)$$

ASSOCIATED CONTENT

Supporting Information

Additional experimental procedures, amino acid sequences of proteins, characterization data, imaging data, analyzed data. The Supporting Information is available free of charge at https://pubs.acs.org/doi/10.1021/jacsau.4c01017.

Additional experimental procedures, amino acid sequences of proteins, characterization data, imaging data, analyzed data (PDF)

Movie S1. A movie that illustrates the motility of microtubule aster-like structures formed by tetrameric TP-Dronpa (AVI)

Movie S2. A movie that illustrates the motility of microtubules with monomeric TP-Dronpa (AVI)

Movie S3. A movie that illustrates the motility of microtubules after conversion of TP-Dronpa-bound microtubules from tetrameric to monomeric state by 505 nm light irradiation for 60 min (AVI)

Movie S4. A movie that illustrates the motility of microtubules after conversion of TP-Dronpa-bound microtubules from monomeric to tetrameric state by 405 nm light irradiation for 30 s (AVI)

Movie S5. A movie that illustrates the motility of tetrameric TP-Dronpa-incorporated microtubules (left) and monomeric TP-Dronpa-incorporated microtubules (right) under depletion condition (AVI)

Movie S6. A movie that illustrates the motility of microtubules with monomeric TP-Dronpa for 5 min, and then the sample was irradiated at 405 nm for 30 s (AVI)

AUTHOR INFORMATION

Corresponding Authors

Hiroshi Inaba − *Department of Chemistry and Biotechnology, Graduate School of Engineering, Tottori University, Tottori 680-8552, Japan; Center for Research on Green Sustainable Chemistry, Tottori University, Tottori 680-8552, Japan;* orcid.org/0000-0002-7658-7827; Email: hinaba@tottori-u.ac.jp

Muneyoshi Ichikawa − *State Key Laboratory of Genetic Engineering, Department of Biochemistry and Biophysics, School of Life Sciences, Fudan University, Shanghai 200438, China;* orcid.org/0000-0002-5921-7699; Email: ichikawa_muneyoshi@fudan.edu.cn

Kazunori Matsuura − *Department of Chemistry and Biotechnology, Graduate School of Engineering, Tottori University, Tottori 680-8552, Japan; Center for Research on Green Sustainable Chemistry, Tottori University, Tottori 680-8552, Japan;* orcid.org/0000-0001-5472-7860; Email: ma2ra-k@tottori-u.ac.jp

Authors

Soei Watari − *Department of Chemistry and Biotechnology, Graduate School of Engineering, Tottori University, Tottori 680-8552, Japan*

Qianru H. Lv − *State Key Laboratory of Genetic Engineering, Department of Biochemistry and Biophysics, School of Life Sciences, Fudan University, Shanghai 200438, China*

Takashi Iwasaki − *Department of Bioresources Science, Graduate School of Agricultural Sciences, Tottori University, Tottori 680-8553, Japan*

Bingxun Wang − *School of Life Science and Technology, ShanghaiTech University, Shanghai 201210, China*

Hisashi Tadakuma − *School of Life Science and Technology, ShanghaiTech University, Shanghai 201210, China;* orcid.org/0000-0002-7877-2559

Akira Kakugo − *Department of Physics and Astronomy, Graduate School of Science, Kyoto University, Kyoto 606-8502, Japan*

Complete contact information is available at: https://pubs.acs.org/10.1021/jacsau.4c01017

Author Contributions

CRediT: **Soei Watari** conceptualization, investigation, methodology, validation, writing - original draft, writing - review & editing; **Hiroshi Inaba** conceptualization, funding acquisition, investigation, methodology, supervision, validation, writing - original draft, writing - review & editing; **Qianru H. Lv**

https://doi.org/10.1021/jacsau.4c01017
JACS Au 2025, 5, 791−801

investigation, methodology, validation, writing - original draft, writing - review & editing; **Muneyoshi Ichikawa** conceptualization, funding acquisition, investigation, methodology, validation, writing - original draft, writing - review & editing; **Takashi Iwasaki** investigation, methodology, validation, writing - original draft, writing - review & editing; **Bingxun Wang** investigation, methodology, validation, writing - original draft, writing - review & editing; **Hisashi Tadakuma** conceptualization, investigation, methodology, validation, writing - original draft, writing - review & editing; **Akira Kakugo** conceptualization, investigation, methodology, writing - original draft, writing - review & editing; **Kazunori Matsuura** conceptualization, investigation, methodology, project administration, supervision, validation, writing - original draft, writing - review & editing.

Notes

The authors declare no competing financial interest.

■ ACKNOWLEDGMENTS

We thank a technical staff Ms. Noriko Matsuura from Tottori University for the help of protein purification, the technical staff of the Chemical Bio-Life Division, Technical Department, Tottori University for technical assistance, and Bio-Electron Microscopy Facility of ShanghaiTech University for TEM imaging. This study was financially supported by FOREST Program (JPMJFR2034) and ACT-X (JPMJAX2012) from the Japan Science and Technology Agency (JST) and the Japan Society for the Promotion of Science (JSPS) KAKENHI Grant number JP23K04931 and JP24H01721 in a Grant-in-Aid for Transformative Research Areas "Materials Science of Meso-Hierarchy" from JSPS to H.I., and by JST, PRESTO (JPMJPR20E1) and Natural Science Foundation of Shanghai (24ZR1403800) to M.I. We thank Edanz (https://jp.edanz.com/ac) for editing a draft of this manuscript.

■ REFERENCES

(1) Akhmanova, A.; Steinmetz, M. O. Control of Microtubule Organization and Dynamics: Two Ends in the Limelight. *Nat. Rev. Mol. Cell Biol.* **2015**, *16*, 711−726.
(2) Brouhard, G. J.; Rice, L. M. Microtubule Dynamics: An Interplay of Biochemistry and Mechanics. *Nat. Rev. Mol. Cell Biol.* **2018**, *19*, 451−463.
(3) McKenna, E. D.; Sarbanes, S. L.; Cummings, S. W.; Roll-Mecak, A. The Tubulin Code, from Molecules to Health and Disease. *Annu. Rev. Cell Dev. Biol.* **2023**, *39*, 331−361.
(4) Atkins, M.; Nicol, X.; Fassier, C. Microtubule Remodelling as a Driving Force of Axon Guidance and Pruning. *Semin. Cell Dev. Biol.* **2023**, *140*, 35−53.
(5) Conde, C.; Cáceres, A. Microtubule Assembly, Organization and Dynamics in Axons and Dendrites. *Nat. Rev. Neurosci.* **2009**, *10*, 319−332.
(6) Stepanek, L.; Pigino, G. Microtubule Doublets Are Double-Track Railways for Intraflagellar Transport Trains. *Science* **2016**, *352*, 721−724.
(7) Ichikawa, M.; Bui, K. H. Microtubule Inner Proteins: A Meshwork of Luminal Proteins Stabilizing the Doublet Microtubule. *BioEssays* **2018**, *40*, No. 1700209.
(8) Ichikawa, M.; Khalifa, A. A. Z.; Kubo, S.; Dai, D.; Basu, K.; Maghrebi, M. A. F.; Vargas, J.; Bui, K. H. Tubulin Lattice in Cilia Is in a Stressed Form Regulated by Microtubule Inner Proteins. *Proc. Natl. Acad. Sci. U.S.A.* **2019**, *116*, 19930−19938.
(9) Burute, M.; Kapitein, L. C. Cellular Logistics: Unraveling the Interplay Between Microtubule Organization and Intracellular Transport. *Annu. Rev. Cell Dev. Biol.* **2019**, *35*, 29−54.
(10) Hess, H.; Ross, J. L. Non-Equilibrium Assembly of Microtubules: From Molecules to Autonomous Chemical Robots. *Chem. Soc. Rev.* **2017**, *46*, 5570−5587.
(11) Needleman, D.; Dogic, Z. Active Matter at the Interface between Materials Science and Cell Biology. *Nat. Rev. Mater.* **2017**, *2*, No. 17048.
(12) Saper, G.; Hess, H. Synthetic Systems Powered by Biological Molecular Motors. *Chem. Rev.* **2020**, *120*, 288−309.
(13) Kabir, A. M. R.; Md, R.; Inoue, D.; Kakugo, A. Molecular Swarm Robots: Recent Progress and Future Challenges. *Sci. Technol. Adv. Mater.* **2020**, *21*, 323−332.
(14) Matsuura, K.; Inaba, H. Photoresponsive Peptide Materials: Spatiotemporal Control of Self-Assembly and Biological Functions. *Biophys. Rev.*. **2023**, *4*, No. 041303.
(15) Keya, J. J.; Suzuki, R.; Kabir, A. M. R.; Inoue, D.; Asanuma, H.; Sada, K.; Hess, H.; Kuzuya, A.; Kakugo, A. DNA-Assisted Swarm Control in a Biomolecular Motor System. *Nat. Commun.* **2018**, *9*, No. 453.
(16) Akter, M.; Keya, J. J.; Kayano, K.; Kabir, A. M. R.; Inoue, D.; Hess, H.; Sada, K.; Kuzuya, A.; Asanuma, H.; Kakugo, A. Cooperative Cargo Transportation by a Swarm of Molecular Machines. *Sci. Robot.* **2022**, *7*, No. eabm0677.
(17) Kawamata, I.; Nishiyama, K.; Matsumoto, D.; Ichiseki, S.; Keya, J. J.; Okuyama, K.; Ichikawa, M.; Kabir, A.; Md, R.; Sato, Y.; Inoue, D.; Murata, S.; Sada, K.; Kakugo, A.; Nomura, S. M. Autonomous Assembly and Disassembly of Gliding Molecular Robots Regulated by a DNA-Based Molecular Controller. *Sci. Adv.* **2024**, *10*, No. eadn4490.
(18) Lemma, L. M.; Varghese, M.; Ross, T. D.; Thomson, M.; Baskaran, A.; Dogic, Z. Spatio-Temporal Patterning of Extensile Active Stresses in Microtubule-Based Active Fluids. *PNAS Nexus* **2023**, *2*, No. pgad130.
(19) Inaba, H.; Yamamoto, T.; Kabir, A.; Md, R.; Kakugo, A.; Sada, K.; Matsuura, K. Molecular Encapsulation Inside Microtubules Based on Tau-Derived Peptides. *Chem. - Eur. J.* **2018**, *24*, 14958−14967.
(20) Inaba, H.; Matsuura, K. Modulation of Microtubule Properties and Functions by Encapsulation of Nanomaterials Using a Tau-Derived Peptide. *Bull. Chem. Soc. Jpn.* **2021**, *94*, 2100−2112.
(21) Watari, S.; Inaba, H.; Tamura, T.; Kabir, A. M. R.; Kakugo, A.; Sada, K.; Hamachi, I.; Matsuura, K. Light-Induced Stabilization of Microtubules by Photo-Crosslinking of a Tau-Derived Peptide. *Chem. Commun.* **2022**, *58*, 9190−9193.
(22) Inaba, H.; Sakaguchi, M.; Watari, S.; Ogawa, S.; Kabir, A.; Md, R.; Kakugo, A.; Sada, K.; Matsuura, K. Reversible Photocontrol of Microtubule Stability by Spiropyran-Conjugated Tau-Derived Peptides. *ChemBioChem* **2023**, *24*, No. e202200782.
(23) Inaba, H.; Sueki, Y.; Ichikawa, M.; Kabir, A.; Md, R.; Iwasaki, T.; Shigematsu, H.; Kakugo, A.; Sada, K.; Tsukazaki, T.; Matsuura, K. Generation of Stable Microtubule Superstructures by Binding of Peptide-Fused Tetrameric Proteins to inside and Outside. *Sci. Adv.* **2022**, *8*, No. eabq3817.
(24) Ando, R.; Mizuno, H.; Miyawaki, A. Regulated Fast Nucleocytoplasmic Shuttling Observed by Reversible Protein Highlighting. *Science* **2004**, *306*, 1370−1373.
(25) Mizuno, H.; Mal, T. K.; Walchli, M.; Kikuchi, A.; Fukano, T.; Ando, R.; Jeyakanthan, J.; Taka, J.; Shiro, Y.; Ikura, M.; Miyawaki, A. Light-Dependent Regulation of Structural Flexibility in a Photochromic Fluorescent Protein. *Proc. Natl. Acad. Sci. U.S.A.* **2008**, *105*, 9227−9232.
(26) Zhou, X. X.; Chung, H. K.; Lam, A. J.; Lin, M. Z. Optical Control of Protein Activity by Fluorescent Protein Domains. *Science* **2012**, *338*, 810−814.
(27) Song, D.; Jo, Y.; Choi, J.-M.; Jung, Y. Client Proximity Enhancement Inside Cellular Membrane-Less Compartments Governed by Client-Compartment Interactions. *Nat. Commun.* **2020**, *11*, No. 5642.
(28) Lyu, S.; Fang, J.; Duan, T.; Fu, L.; Liu, J.; Li, H. Optically Controlled Reversible Protein Hydrogels Based on Photoswitchable Fluorescent Protein Dronpa. *Chem. Commun.* **2017**, *53*, 13375−13378.

https://doi.org/10.1021/jacsau.4c01017
JACS Au 2025, 5, 791−801

(29) Wu, X.; Huang, W.; Wu, W.-H.; Xue, B.; Xiang, D.; Li, Y.; Qin, M.; Sun, F.; Wang, W.; Zhang, W.-B.; Cao, Y. Reversible Hydrogels with Tunable Mechanical Properties for Optically Controlling Cell Migration. *Nano Res.* **2018**, *11*, 5556−5565.
(30) Mizuno, H.; Dedecker, P.; Ando, R.; Fukano, T.; Hofkens, J.; Miyawaki, A. Higher Resolution in Localization Microscopy by Slower Switching of a Photochromic Protein. *Photochem. Photobiol. Sci.* **2010**, *9*, 239−248.
(31) Zhou, X. X.; Fan, L. Z.; Li, P.; Shen, K.; Lin, M. Z. Optical Control of Cell Signaling by Single-Chain Photoswitchable Kinases. *Science* **2017**, *355*, 836−842.
(32) Schmidt-Cernohorska, M.; Zhernov, I.; Steib, E.; Le Guennec, M.; Achek, R.; Borgers, S.; Demurtas, D.; Mouawad, L.; Lansky, Z.; Hamel, V.; Guichard, P. Flagellar Microtubule Doublet Assembly in Vitro Reveals a Regulatory Role of Tubulin C-Terminal Tails. *Science* **2019**, *363*, 285−288.
(33) Inoue, D.; Mahmot, B.; Kabir, A. M. R.; Farhana, T. I.; Tokuraku, K.; Sada, K.; Konagaya, A.; Kakugo, A. Depletion Force Induced Collective Motion of Microtubules Driven by Kinesin. *Nanoscale* **2015**, *7*, 18054−18061.

https://doi.org/10.1021/jacsau.4c01017
JACS Au 2025, 5, 791−801